

# Structural and magnetic properties of $\text{Ho}_5(\text{Si}_x\text{Ge}_{1-x})_4$

A. M. Pereira, J. B. Sousa, and J. P. Araujo\*  
 IFIMUP, Rua do Campo Alegre, 678, 4169-007 Porto, Portugal

C. Magen  
 CEMES-CNRS/Nanomat, Boîte Postale 4347, 31055 Toulouse, France

P. A. Algarabel  
 Instituto de Ciencia de Materiales de Aragón, Universidad de Zaragoza and Consejo Superior de Investigaciones Científicas,  
 50009 Zaragoza, Spain

L. Morellon, C. Marquina, and M. R. Ibarra  
 Instituto de Ciencia de Materiales de Aragón, Universidad de Zaragoza and Consejo Superior de Investigaciones Científicas,  
 50009 Zaragoza, Spain

and Instituto de Nanociencia de Aragón, Universidad de Zaragoza, 50009 Zaragoza, Spain

(Received 14 December 2007; revised manuscript received 20 February 2008; published 2 April 2008)

The crystal structure, phase relationship, and magnetic properties of the system  $\text{Ho}_5(\text{Si}_x\text{Ge}_{1-x})_4$  have been studied using polycrystalline samples with compositions  $x=0, 0.25, 0.5, 0.75, 0.875$ , and 1. At room temperature, the concentration range  $0 \leq x \leq 0.5$  presents an orthorhombic  $\text{Sm}_5\text{Ge}_4$ -type  $O(\text{II})$  structure, whereas the monoclinic  $M$  phase sets in the compounds with concentrations  $x=0.75$  and  $0.875$ . The orthorhombic  $\text{Gd}_5\text{Si}_4$ -type  $O(\text{I})$  structure is present only for  $x=1$ . Magnetic characterization has shown that the  $\text{Ho}_5(\text{Si}_x\text{Ge}_{1-x})_4$  system is paramagnetic at 300 K. The samples with an  $O(\text{II})$  structure undergo a second order antiferromagnetic transition with  $T_N$  between 25 and 30 K. The compounds with  $x > 0.5$  present a low temperature ferromagnetic phase with  $T_C$  rapidly increasing with Si content ( $dT_C/dx=95$  K). A second magnetic transition has been detected in the whole composition range at  $T_{SR} \sim 15$  K, which might correspond to a reorientation of the easy magnetization axis. Linear thermal expansion experiments evidence no spontaneous structural transition with the exception of  $\text{Ho}_5\text{Ge}_4$ , where a small anomaly has been observed, which is probably due to the structural change of a small fraction of the sample volume.

DOI: [10.1103/PhysRevB.77.134404](https://doi.org/10.1103/PhysRevB.77.134404)

PACS number(s): 75.30.Sg, 81.30.Bx, 75.30.Kz, 61.66.-f

## I. INTRODUCTION

The magnetocaloric effect (MCE) has been extensively studied in the past years, especially after Pecharsky and Gschneidner<sup>1</sup> discovered a giant MCE between 270 and 300 K in the  $\text{Gd}_5\text{Si}_2\text{Ge}_2$  compound. This finding and its potential application on room temperature magnetic refrigeration technology<sup>2-5</sup> induced a renewed interest on the  $R_5(\text{Si}_x\text{Ge}_{1-x})_4$  family of compounds ( $R$ =rare earth),<sup>6-19</sup> leading to the discovery of many other peculiar physical properties, namely, unusual magnetostructural transitions,<sup>20</sup> giant magnetoresistance<sup>4,21</sup> and other exotic electrical properties,<sup>22-26</sup> giant magnetostriction,<sup>27,28</sup> and more recently a Griffiths-like behavior observed in some Gd (Ref. 29) and Tb (Ref. 30) compounds. Additionally, these structural, magnetic, and electrical properties were found to strongly depend on Si/Ge concentration ( $x$ ), giving rise to very complex phase diagrams reflecting the strong interplay between lattice, charge, and spin degrees of freedom.<sup>3,10,12,22,24,31</sup>

In spite of this effort, scarce information is known about the  $R$ =Ho compounds. Holtzberg *et al.*<sup>32</sup> were the first to study the structural and magnetic properties of  $\text{Ho}_5\text{Ge}_4$ . They found that this compound crystallizes in the  $\text{Sm}_5\text{Ge}_4$ -type  $Pnma$  orthorhombic structure with 4 f.u./unit cell and exhibits a second order paramagnetic (PM) to antiferromagnetic (AFM) phase transition at  $T_N=21$  K. From the reciprocal

magnetic susceptibility, a positive paramagnetic Curie-Weiss temperature of  $\Theta_p=16$  K was obtained, revealing the presence of ferromagnetic (FM) interactions due to the Rudermann-Kittel-Kasuya-Yosida exchange interactions between Ho ions.<sup>32</sup> Afterward, by using neutron diffraction experiments, Schobinger-Papamantellos and Niggli<sup>33</sup> observed a change on the easy magnetization axis at  $T=18$  K.<sup>33</sup> Holtzberg *et al.*<sup>32</sup> also characterized the compound  $\text{Ho}_5\text{Si}_4$  and showed that at room temperature, it is PM and crystallizes in a  $\text{Gd}_5\text{Si}_4$ -type  $Pnma$  structure. At low temperatures, a second order FM transition occurs at  $T_C=76$  K. A recent work by Thuy *et al.*<sup>34</sup> claims that  $\text{Ho}_5\text{Si}_2\text{Ge}_2$  also exhibits a  $Pnma$  structure at 300 K and an AFM phase transition at  $T_N=25$  K, although in this case, a drastic increase in the magnetization was observed when an external magnetic field is applied ( $H \sim 12$  kOe) at 5 K and attributed to a metamagnetic phase transition.

In the present work, we report a detailed structural [x-ray diffraction and scanning electron microscopy (SEM)], magnetic [superconducting quantum interference device (SQUID) magnetometry], and magnetoelastic [linear thermal expansion (LTE) and magnetostriction] study of the  $\text{Ho}_5(\text{Si}_x\text{Ge}_{1-x})_4$  system, with  $x=0, 0.25, 0.5, 0.75, 0.875$ , and 1. As a result, the magnetic and structural  $x$ - $T$  phase diagram is proposed.

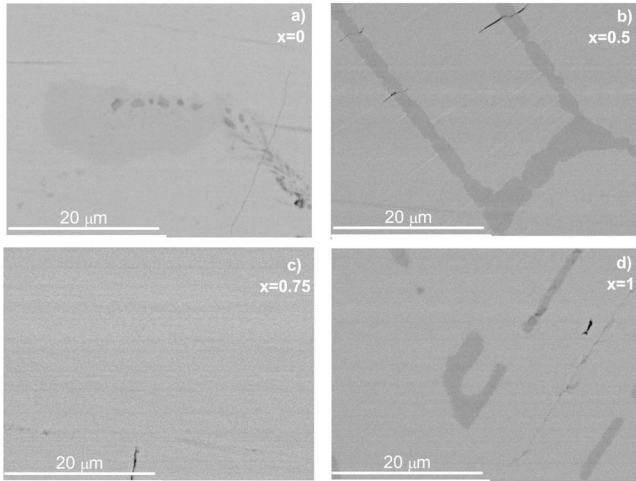


FIG. 1. Backscattered electron SEM micrographs of samples with  $x=0, 0.5, 0.75,$  and  $1.$

## II. EXPERIMENTAL DETAILS

Polycrystalline specimens of  $\text{Ho}_5(\text{Si}_x\text{Ge}_{1-x})_4$ , with  $x=0, 0.25, 0.5, 0.75, 0.875,$  and  $1,$  were synthesized by arc melting of stoichiometric mixtures of high-purity Ho (99.99 wt %) and Si and Ge (99.9999 wt %). Weight losses during melting were negligible, and therefore, the initial compositions were assumed unchanged.

The quality of the as-cast samples was checked by x-ray powder diffraction and SEM combined with x-ray energy dispersive spectrometry (EDS). The crystallographic structure was determined by Rietveld refinement of the x-ray diffraction patterns using the software package FULLPROF.<sup>35</sup> Magnetization experiments were performed in a commercial (Quantum Design) SQUID magnetometer in the temperature range of 5–300 K and magnetic fields up to 50 kOe. Linear thermal expansion and magnetostriction measurements were performed using the strain gauge technique from 10 to 300 K.<sup>36</sup>

## III. EXPERIMENTAL RESULTS

### A. Structural characterization

Figure 1 displays several backscattered electron SEM micrographs of samples with  $x=0, 0.5, 0.75,$  and  $1.$  These images have been selected to illustrate the regions of the sample where the secondary phases are found and they are not representative of the phase abundance in the sample. EDS analysis has shown that the composition of the matrix is very close to the nominal one in all samples. Whereas in the sample with  $x=0.75$  no evidence of impurities is observed [see Fig. 1(c)], the other compounds show small traces of areas lighter (higher atomic mass) and darker (lower atomic mass) than the  $\text{Ho}_5(\text{Si},\text{Ge})_4$  matrix. The stoichiometry of these areas corresponds to the impurity phases  $\text{Ho}_5(\text{Si},\text{Ge})_3$  and  $\text{Ho}(\text{Si},\text{Ge}),$  respectively, which are usual in the 5:4 compounds. In order to determine the crystallographic structure, i.e., lattice parameters, and to quantify the amount of the secondary phases, we have performed Rietveld refinements

TABLE I. Room temperature crystalline structure and cell parameters for the  $\text{Ho}_5(\text{Si}_x\text{Ge}_{1-x})_4$  system.

$x$	Structure	$a$	$b$	$c$	$\beta$
0	$Pnma$ [ $\text{Sm}_5\text{Ge}_4, O(\text{II})$ ]	7.565(3)	14.549(1)	7.636(4)	
0.25	$Pnma$ [ $\text{Sm}_5\text{Ge}_4, O(\text{II})$ ]	7.531(0)	14.537(3)	7.610(1)	
0.5	$Pnma$ [ $\text{Sm}_5\text{Ge}_4, O(\text{II})$ ]	7.517(9)	14.535(4)	7.601(3)	
0.75	$P112_1/a$ [ $\text{Gd}_5\text{Si}_2\text{Ge}_2, M$ ]	7.428(2)	14.498(9)	7.624(5)	93.003(8)
0.875	$P112_1/a$ ( $\text{Gd}_5\text{Si}_2\text{Ge}_2, M$ )	7.425(6)	14.486(1)	7.605(5)	93.084(1)
1	$Pnma$ [ $\text{Gd}_5\text{Si}_4, O(\text{I})$ ]	7.340(9)	14.470(1)	7.639(4)	

of the room temperature x-ray diffraction patterns. The results of the fits are summarized in Table I, and as an illustrative example, the refinement for the compound  $\text{Ho}_5(\text{Si}_{0.25}\text{Ge}_{0.75})_4$  is displayed in Fig. 2. In full correspondence with the EDS analysis, the amount of secondary phases estimated is always less than 10%, and in the case of  $x=0.75$  composition, the refinement can be performed assuming the presence of a single 5:4 phase.<sup>38</sup>

The analysis of the x-ray powder diffraction data reveals that the pseudobinary  $\text{Ho}_5(\text{Si}_x\text{Ge}_{1-x})_4$  system presents three distinct crystal structures at room temperature as a function of the composition. The holmium silicide crystallizes in the  $Pnma$  orthorhombic space group with the  $\text{Gd}_5\text{Si}_4$ -type [ $O(\text{I})$ ] structure. The samples in the composition range  $0.75 \leq x \leq 0.85$  exhibit a monoclinic  $\text{Gd}_5\text{Si}_2\text{Ge}_2$ -type ( $M$ ) structure, which belongs to the  $P112_1/a$  space group. Finally, the Gerich compounds ( $x \leq 0.5$ ) adopt the orthorhombic  $\text{Sm}_5\text{Ge}_4$ -type [ $O(\text{II})$ ] structure, which also belongs to the  $Pnma$  space group.<sup>27</sup>

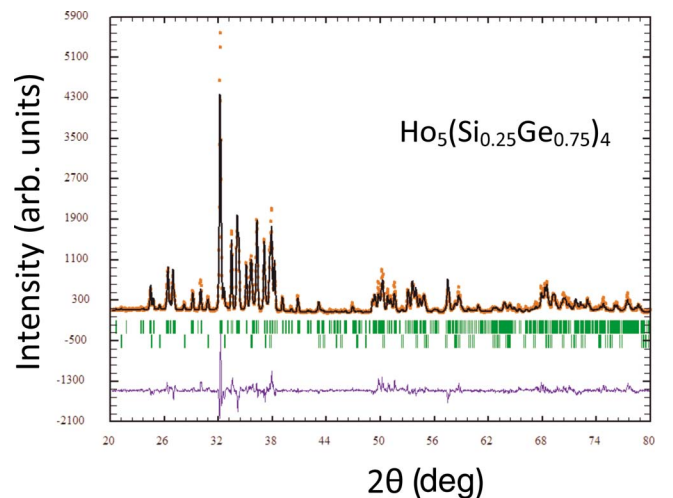


FIG. 2. (Color online)  $\theta$ - $2\theta$  x-ray diffraction for  $\text{Ho}_5(\text{Si}_{0.25}\text{Ge}_{0.75})_4$  from  $20^\circ$  to  $80^\circ$  in steps of  $0.03^\circ$  at room temperature.

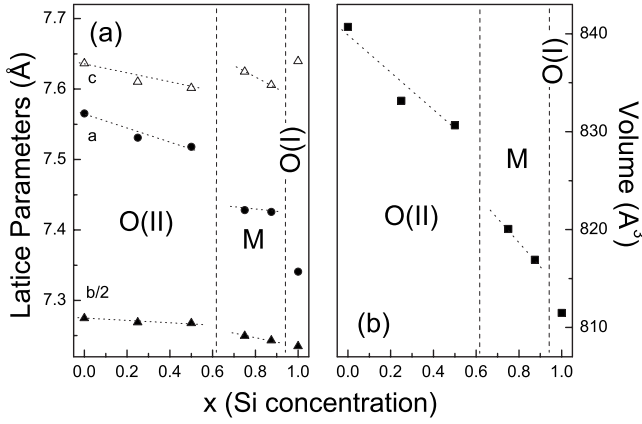


FIG. 3. (a) Lattice parameters and (b) unit cell volume of  $\text{Ho}_5(\text{Si}_x\text{Ge}_{1-x})_4$  as a function of  $x$  at 300 K.

The dependence of the lattice parameters and the unit cell volume on the Si concentration ( $x$ ) at room temperature is shown in Figs. 3(a) and 3(b), respectively. By observing Fig. 3(a), one notices that, in general, the lattice parameters tend to moderately decrease with Si doping within each solid solution region. The drastic changes occur when changing the crystal structure. In this case, the  $a$  parameter drastically decreases, which is about  $-1.2\%$  and  $-1.1\%$  in the phase changes  $O(\text{I}) \rightarrow M$  and  $M \rightarrow O(\text{II})$ , respectively. The lattice parameters  $b$  and  $c$  experiment rather moderate changes,  $\Delta b/b \cong +0.3\%$  and  $\Delta c/c \cong -0.3\%$  in the phase boundary  $O(\text{I}) \rightarrow M$  and  $\Delta b/b \cong +0.3\%$  and  $\Delta c/c \cong -0.1\%$  in  $M \rightarrow O(\text{II})$  [Fig. 3(a)]. Therefore, the change in crystallographic structure induces remarkable lattice changes.

As one can see in Fig. 3(b), the overall effect of Si on substituting Ge for the smaller Si atom is that of reducing the unit cell volume, both within each solid solution region and in the induced crystal changes,  $\Delta V/V \cong -1.2\%$  in  $O(\text{I}) \rightarrow M$  and  $\Delta V/V \cong -1.0\%$  in  $M \rightarrow O(\text{II})$ .

We can predict the type of crystal structure for a compound with a specific  $x$  concentration by taking the coefficient between the different radius ( $f_r$ ) of magnetic ( $r_R$ ) and nonmagnetic ( $r_T$ ) atoms into consideration.<sup>17</sup>

In a previous work, Pecharsky *et al.*<sup>17</sup> established a correlation between the crystal structure of the  $R_5(\text{Si}_x\text{Ge}_{1-x})_4$  alloys and the ratio between the radius of magnetic ( $r_R$ ) and nonmagnetic ( $r_T$ ) atoms, i.e.,  $f_r = r_R/r_T$ . In this phenomenological study, the  $\text{Gd}_5\text{Si}_4$ -type  $O(\text{I})$  structural phase is found for values of  $f_r$  between 1.370 and 1.334, the  $\text{Gd}_5\text{Si}_2\text{Ge}_2$ -type  $M$  structure is expected between 1.333 and 1.326, and the  $\text{Sm}_5\text{Ge}_4$ -type  $O(\text{II})$  structure falls in the range of 1.319–1.290. We can predict the type of crystal structure given by this model considering that  $r_R$  is the metallic radius of Ho ( $r_R = 1.776 \text{ \AA}$ ) (Ref. 37) and  $r_T$  is obtained as a weighted average radius that is given by the statistical molar fraction of Si ( $f_{\text{Si}}$ ) and the different radii of Si and Ge ( $r_{\text{Si}} = 1.322 \text{ \AA}$  and  $r_{\text{Ge}} = 1.378 \text{ \AA}$  from Ref. 17),

$$r_T = f_{\text{Si}}r_{\text{Si}} + (1 - f_{\text{Si}})r_{\text{Ge}}. \quad (1)$$

Table II displays the values of  $f_r$  obtained for the  $\text{Ho}_5(\text{Si}_x\text{Ge}_{1-x})_4$  compounds and their corresponding crystal

TABLE II. Phenomenological crystallographic phase prediction for the  $\text{Ho}_5(\text{Si}_x\text{Ge}_{1-x})_4$  system.

$x$	$r_R/r_T$	Phase
0.00	1.282	$O(\text{II})$
0.25	1.295	$O(\text{II})$
0.50	1.308	$O(\text{II})$
0.75	1.322	$M$
0.875	1.326	$M$
1.00	1.336	$O(\text{I})$

structures, showing good agreement with the model of Pecharsky *et al.* (Ref. 17).

### B. Linear thermal expansion

Temperature dependence of the LTE for several representative specimens of  $\text{Ho}_5(\text{Si}_x\text{Ge}_{1-x})_4$  in the temperature range of 10–300 K is depicted in Fig. 4.  $\text{Ho}_5\text{Ge}_4$  exhibits a small LTE anomaly ( $\Delta l/l \sim 0.01\%$ ) at  $T \sim 27 \text{ K}$ , as can be observed in the inset, which is the usual signal of the occurrence of a structural transition. However, the magnitude of this step is about 0.01%, which is an order of magnitude smaller than typical LTE discontinuities of about 0.1%–0.3%, characteristic of a structural transition in polycrystalline specimens. This fact points to the possibility of a partial structural transformation, which is confirmed by the measurement of magnetostriction (MS) upon pulsed magnetic fields in the vicinity of the LTE anomaly, as shown in the inset of Fig. 4. In this case, a large anomaly of about  $-0.18\%$  is induced at a magnetic field of 20 kOe. It is worth mentioning that this transition does not show significant hysteretic behavior both at the  $M(H)$  isotherms and at the pulsed field MS. Further studies are now needed to clarify the nature of this anomaly, which is likely associated, as in other 5:4

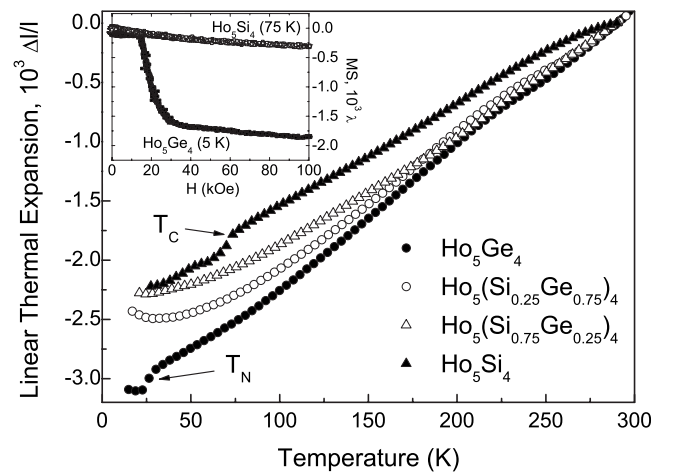


FIG. 4. Temperature dependence of the LTE of the  $\text{Ho}_5(\text{Si}_x\text{Ge}_{1-x})_4$  samples, with  $x = 0, 0.25, 0.75,$  and  $1$ , in the temperature range of 10–300 K. Inset: MS upon pulsed magnetic fields in the vicinity of the LTE anomaly for  $\text{Ho}_5\text{Ge}_4$  and  $\text{Ho}_5\text{Si}_4$  at  $T = 5 \text{ K}$  and  $T = 75 \text{ K}$ , respectively.

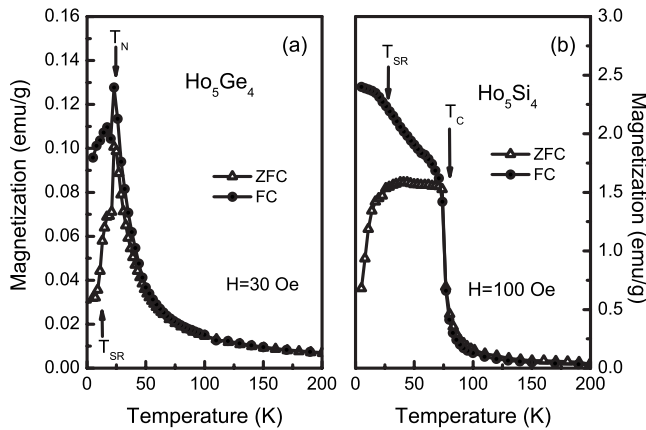


FIG. 5. ZFC-FC magnetization curves of (a)  $\text{Ho}_5\text{Ge}_4$  measured with a 30 Oe applied magnetic field and (b)  $\text{Ho}_5\text{Si}_4$  with a magnetic field of 100 Oe in the temperature range of 5–200 K.

compounds, with a field induced structural transformation to a high field  $O(I)$  phase.<sup>13</sup>

For the  $x=0.25$  and  $0.75$  compounds, the temperature dependence of LTE follows a typical Gruneisen law showing no structural transition, but the  $\text{Ho}_5\text{Si}_4$  compound exhibits a small kink at  $T_C=71$  K, which could be related to lattice instabilities induced by the ferromagnetic ordering that is similar to a comparable anomaly found in  $\text{Er}_5\text{Si}_4$  upon high pressure.<sup>40</sup> The MS measurement plotted in the inset of Fig. 4 points to the absence of any structural transformation associated with the magnetic transition.

### C. Magnetization

Magnetic characterization of the  $\text{Ho}_5(\text{Si}_x\text{Ge}_{1-x})_4$  system is illustrated in Figs. 5–8. Zero-field-cooling (ZFC) and field-cooling (FC) magnetization experiments in all the samples studied are plotted in Figs. 5–7, whereas magnetization isotherms at 5 K up to 50 kOe are pictured in Fig. 8.

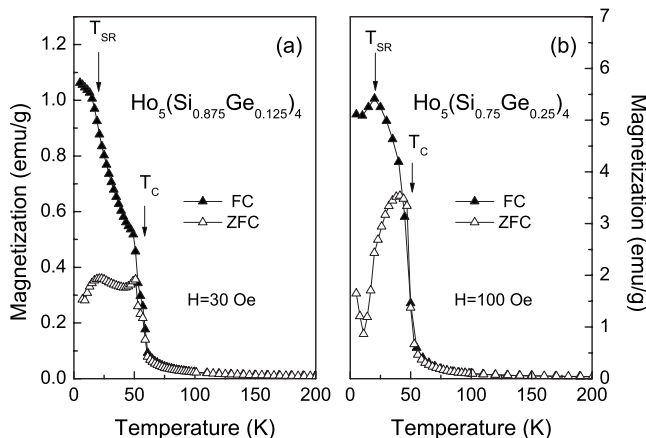


FIG. 6. ZFC-FC magnetization curves of (a)  $\text{Ho}_5(\text{Si}_{0.875}\text{Ge}_{0.125})_4$  measured with a 30 Oe applied magnetic field and (b)  $\text{Ho}_5(\text{Si}_{0.75}\text{Ge}_{0.25})_4$  with a magnetic field of 100 Oe in the temperature range of 5–300 K.

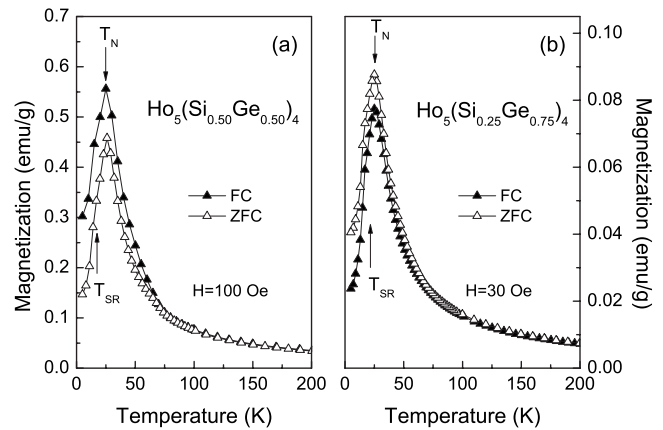


FIG. 7. ZFC-FC magnetization curves of (a)  $\text{Ho}_5(\text{Si}_{0.5}\text{Ge}_{0.5})_4$  measured with a 100 Oe applied magnetic field and (b)  $\text{Ho}_5(\text{Si}_{0.25}\text{Ge}_{0.75})_4$  with a magnetic field of 30 Oe in the temperature range of 5–300 K.

In Fig. 5(a), the temperature dependence of the magnetization measured with  $H=30$  Oe for  $\text{Ho}_5\text{Ge}_4$  is presented. This picture shows that the  $\text{Ho}_5\text{Ge}_4$  compound is in the AFM magnetic phase at low temperatures, confirming the previous work of Holtzberg *et al.*<sup>32</sup> A sharp peak at  $T_N=25$  K is observed without any hysteresis, confirming the second order nature of the transition. A shoulder at lower temperature  $T_{SR}=18$  K is attributed to a spin reorientation transition and is in agreement with Ref. 33.

Above  $T_N$ , the reciprocal susceptibility shows a typical Curie–Weiss behavior ( $\chi^{-1} = \frac{T-\Theta_p}{C_c}$ , where  $C_c$  is the Curie constant), allowing us to obtain a Curie–Weiss temperature of  $\Theta_p=21$  K and an effective paramagnetic moment per Ho ion of  $\mu_{eff}=8.9\mu_B$ . This value is rather low when compared to the expected theoretical value for the paramagnetic  $\text{Ho}^{3+}$  free ion ( $\mu_{eff}=10.07\mu_B$ ).

Figure 5(b) displays the magnetization ( $M$ ) of  $\text{Ho}_5\text{Si}_4$  in the 5–300 K temperature range in an applied magnetic field

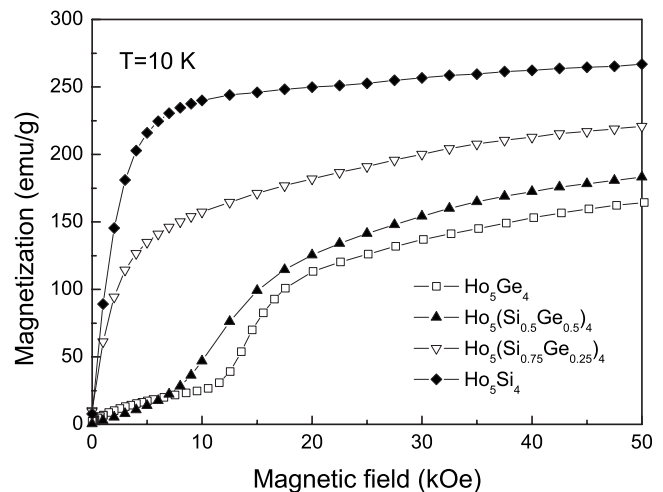


FIG. 8. Magnetization isotherms of  $\text{Ho}_5\text{Si}_4$ ,  $\text{Ho}_5(\text{Si}_{0.75}\text{Ge}_{0.25})_4$ ,  $\text{Ho}_5(\text{Si}_{0.5}\text{Ge}_{0.5})_4$ , and  $\text{Ho}_5\text{Ge}_4$  compounds measured at 10 K in magnetic fields up to 50 kOe.

of  $H=100$  Oe. A ferromagneticlike order is seen at low temperatures with a Curie temperature  $T_C=77$  K. No thermal hysteresis was observed between heating and cooling curves, as characteristic of second order transitions.

A secondary shoulder is found at  $T_{SR}\sim 17$  K, which can be associated with a spin reorientation transition that is similar to the one found in the  $\text{Tb}_5\text{Si}_4$  compound.<sup>10</sup> These transitions are usually a consequence of the large magnetocrystalline anisotropy present in some rare earth ions and can be observed from the ZFC and FC differences. Above  $T_C$ , the effective paramagnetic moment obtained is  $\mu_{eff}\sim 10.0\mu_B$ , which is in good agreement with the expected theoretical value.

We measured the temperature dependence of magnetization of the  $\text{Ho}_5(\text{Si}_{0.875}\text{Ge}_{0.125})_4$  [Fig. 6(a)] and  $\text{Ho}_5(\text{Si}_{0.75}\text{Ge}_{0.25})_4$  [Fig. 6(b)] compounds with applied magnetic fields  $H=30$  Oe and  $H=100$  Oe, respectively. At low temperatures, ferromagnetic orders are seen with Curie temperatures  $T_C=58$  K and  $T_C=49$  K for  $x=0.8$  and  $0.75$ , respectively. Again, no thermal hysteresis is observed near  $T_C$ , revealing the second order nature of the magnetic transition. A shoulder in  $M(T)$  is also observed at  $T_{SR}\sim 15$  K and  $T_{SR}\sim 18$  K (for  $x=0.8$  and  $0.75$ , respectively), which is attributed to a spin reorientation transition, as observed for  $\text{Ho}_5\text{Si}_4$ . By using the Curie–Weiss law and our data in the paramagnetic region, we obtain the following results:  $\Theta_P=33.9$  K and  $\mu_{eff}=9.9\mu_B$  and  $\Theta_P=32.7$  K and  $\mu_{eff}=10.1\mu_B$ , for  $\text{Ho}_5(\text{Si}_{0.875}\text{Ge}_{0.125})_4$  and  $\text{Ho}_5(\text{Si}_{0.75}\text{Ge}_{0.25})_4$ , respectively.

The  $M(T)$  measurements, which are presented in Fig. 7 for the compounds with concentrations  $x=0.25$  and  $x=0.5$ , reveal that both are in the AFM phase at low temperatures with transition temperatures  $T_N=30$  and  $31$  K, respectively, thus confirming previous results for the  $x=0.5$  compound.<sup>34</sup>

By using the  $\chi^{-1}$  value obtained in the paramagnetic state, we calculate  $\mu_{eff}=11.3\mu_B$  and  $\mu_{eff}=10.2\mu_B$  for the  $x=0.5$  and  $x=0.25$  compounds, respectively. The low positive value of the Curie temperature  $\Theta_P=15$  K suggests the existence of weak FM interactions between the adjacent Ho ion, which is similar to those found in Gd, Tb, and Er compounds.<sup>6,10,13,15,16</sup> In Fig. 8, we represent isotherm magnetization measurements at  $T=10$  K for the compounds with  $x=0, 0.5, 0.75$ , and  $1$ , displaying a complex magnetic behavior. For the AFM samples, a drastic increase in magnetization is observed, suggesting a magnetic transition from an AFM to a FM. This transition occurs at critical field ( $H_C$ ), which decreases with the increase in Si concentration (from  $H_C=14$  kOe for  $x=0$  and until  $H_C=12.6$  kOe for  $x=0.5$ ). This behavior was seen in similar compounds (e.g., in  $\text{Gd}_5\text{Ge}_4$ ).<sup>10</sup> For compounds with  $x=1$  and  $0.75$ , we observed a normal FM behavior with a clear saturation. From these results, we obtain a saturation magnetic moment  $\sigma_S=8.9\mu_B$  and  $7.8\mu_B$  for  $x=1$  and  $0.75$ , which is close to the theoretical value of  $\sigma_S=9.0\mu_B$  ( $gJ$ ). The AFM samples have much smaller values of  $6.7\mu_B$  and  $6.5\mu_B$  for  $x=0.5$  and  $x=0$ , respectively.

$T_C$ ,  $T_N$ ,  $T_{SR}$ ,  $\mu_{eff}$ ,  $\sigma_S$ , and  $\Theta_P$ , which are obtained for all the studied compounds, are summarized in Table III.

TABLE III. Magnetic data for the  $\text{Ho}_5(\text{Si}_x\text{Ge}_{1-x})_4$  system.

$x$	$T_C$ (K)	$T_N$ (K)	$T_{SR1}$ (K)	$\mu_{eff}$ ( $\mu_B$ )	$\sigma_S$ ( $\mu_B$ )	$\Theta_P$ (K)
0		25	18	8.9	6.5	21
0.25		30	15	10.2	6.5	15
0.5		31	15	11.3	6.6	15
0.75	49		18	10.1	7.8	32.7
0.875	57		15	9.9	8.4	33.9
1	77		17	10.0	8.9	40

#### D. Magnetic-structural phase diagram

Based on the experimental results presented so far, we propose a magnetic and crystallographic composition-temperature ( $x$ - $T$ ) phase diagram of the  $\text{Ho}_5(\text{Si}_x\text{Ge}_{1-x})_4$  system, which is displayed in Fig. 9. At room temperature, all compounds are PM and three distinct crystal phases are observed as a function of the composition [i.e.,  $O(\text{II})$ ,  $M$ , and  $O(\text{I})$ ], which is similar to the cases of  $\text{Gd}_5(\text{Si}_x\text{Ge}_{1-x})_4$  and  $\text{Tb}_5(\text{Si}_x\text{Ge}_{1-x})_4$ .<sup>10,27</sup>

The compounds with  $x\leq 0.5$  present an  $O(\text{II})$  structural phase undergoing an AFM ordering at  $T_N$  ranging from 25 K ( $x=0$ ) to 30 K ( $x=0.5$ ). An order-order transition is observed in these compounds that might correspond to a change between two AFM states (from AFM1 to AFM2) around  $T_{SR}\sim 15$  K due to a change on the easy magnetization axis.

The  $M$  phase sets in the composition range  $0.75\leq x\leq 0.875$ , while for  $x>0.875$ , an  $O(\text{I})$  crystallographic phase is found. For all these compounds, a PM-FM transition is observed at  $T_C$  increasing nearly linearly from 49 K ( $x=0.75$ ) to 77 K ( $x=1$ ) at a rate of  $dT_C/dx\sim 95$  K. In this composition range, a pure spin reorientation transition is also observed at  $T_{SR}\sim 18$  K, changing from FM1 to FM2, due to a variation of the easy magnetization direction promoted by the large magnetocrystalline anisotropy of the Ho ion.

Furthermore, this magnetostructural phase diagram follows the Gd, Tb, and Dy features, which show a regular increase in the stability window of the  $\text{Sm}_5\text{Ge}_4$ -type [ $O(\text{II})$ ]

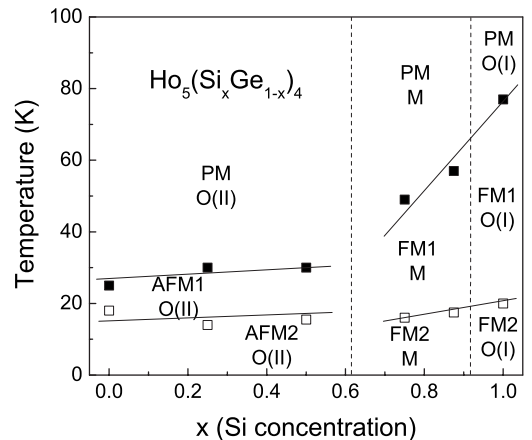


FIG. 9. Magnetic and crystallographic  $x$ - $T$  phase diagram of  $\text{Ho}_5(\text{Si}_x\text{Ge}_{1-x})_4$  in the temperature range of 5–100 K.

structure along the Periodic Table period,<sup>41</sup> privileging the AFM order phase at low temperatures. Most likely, this is due to single-ion anisotropy which prevents long range FM ordering to occur despite a positive Curie–Weiss temperature. Within this picture, the AFM order results from competing FM interactions and anisotropy, giving rise to spiral or conical AFM magnetic structures, which are also characteristic for Tb, Dy, and Ho rare elements.<sup>42</sup>

Our results also confirm that the crystallographic transformations that are observed in the Gd and Tb compounds, which accompany the magnetic transitions and are responsible for the large MCE observed in these compounds, are not present in  $\text{Ho}_5(\text{Si}_x\text{Ge}_{1-x})_4$ .<sup>6,10,15,16</sup>

However, the compound  $\text{Ho}_5\text{Ge}_4$  has shown a small but significant anomaly in the low temperature LTE, which is similar to other singular 5:4 compounds such as  $\text{Gd}_5\text{Ge}_4$ ,<sup>39,40,43</sup> that might indicate the possibility of inducing a complete structural transformation by changing other external parameters such as magnetic field or hydrostatic pressure, and subsequently, a promising high MCE at low temperatures.

#### IV. CONCLUSIONS

In summary, we have carried out a detailed study of the crystallographic and magnetic properties of the  $\text{Ho}_5(\text{Si}_x\text{Ge}_{1-x})_4$  system. Selected compositions clarify that the phase diagram presents three different structure types at 300 K depending on Si concentration. The magnetic properties allowed us to complete the phase diagram (Fig. 9) where no structural transition is observed in the 5–300 K range. The compounds having an  $O(\text{II})$  structure ( $0 < x \leq 0.5$ ) at 300 K are in the PM phase, and for a critical temperature  $T_N$  be-

tween 25 and 30 K, a second order PM-AFM transition occurs. Between  $x=0.75$  and  $x=0.875$ , a purely monoclinic structure is found, which sets below  $T_C$ . The silicide compound crystallizes in the  $\text{Ho}_5\text{Si}_4$  structure having a magnetic transition at  $\text{Ho}_5\text{Si}_4$ , changing to a FM magnetic phase. A second magnetic transition (order-order) is observed at low temperatures in all compounds corresponding to a spin reorientation transition, which is similar to what occurs in the  $\text{Tb}_5(\text{Si}_x\text{Ge}_{1-x})_4$  system<sup>10</sup> and also in the  $\text{Ho}_5\text{Ge}_4$  system.<sup>33</sup> However, macroscopically, the appearance of these anomalies in  $(\text{Gd}_5\text{Si}_2\text{Ge}_2\text{-M})$  data can be enhanced by the precipitates of the spurious phase  $[\text{Ho}_5(\text{Si},\text{Ge})_3, \text{Ho}(\text{Si},\text{Ge})]$  observed by our x-ray and SEM data. To confirm the real nature of the spin reorientation transition and the magnetic structure of  $\text{Ho}_5(\text{Si}_x\text{Ge}_{1-x})_4$  in all compounds, further investigation is in progress, namely, neutron diffraction.

#### ACKNOWLEDGMENTS

This work was supported in part by Project No. POCI/CTM/61284/2004 and Project No. FEDER/POCTI n2–155/94 from Fundacao para a Ciencia e Tecnologia (FCT). André Pereira is thankful for a Ph.D. grant (SFRH/BD/22373/2005) from FCT, Portugal. C.M. would also like to thank the Fundación Ramón Areces for his postdoctoral grant “Beca para ampliación de estudios en universidades y centros de investigación en el extranjero en el campo de las Ciencias de la Naturaleza (2006–2007).” The financial support of the Spanish CICYT under Grant No. MAT2000-1756 is also gratefully acknowledged. The financial support of the Spanish MEC (MAT2005-05565-C02) and DGA (Grant No. E26 and Project No. PIP017/2005) is acknowledged. Part of this work has been supported by EuroMagNET under the EU Contract No. RII3-CT-2004-506239.

\*jearaujo@fc.up.pt

<sup>1</sup>V. K. Pecharsky and K. A. Gschneidner, Jr., *Phys. Rev. Lett.* **78**, 4494 (1997).

<sup>2</sup>V. K. Pecharsky and K. A. Gschneidner, Jr., *Appl. Phys. Lett.* **70**, 3299 (1997).

<sup>3</sup>V. K. Pecharsky and K. A. Gschneider, Jr., *Adv. Cryog. Eng.* **43**, 1729 (1998).

<sup>4</sup>L. Morellon, J. Sankiewicz, B. Garcia-Landa, P. A. Algarabel, and M. R. Ibarra, *Appl. Phys. Lett.* **73**, 3462 (1998).

<sup>5</sup>V. K. Pecharsky and K. A. Gschneider, Jr., *J. Magn. Magn. Mater.* **200**, 44 (1999).

<sup>6</sup>K. A. Gschneidner, Jr., V. K. Pecharsky, A. O. Pecharsky, V. V. Ivchenko, and E. M. Levin, *J. Alloys Compd.* **303-304**, 214 (2000).

<sup>7</sup>W. Choe, V. K. Pecharsky, A. O. Pecharsky, K. A. Gschneidner, Jr., V. G. Young, Jr., and G. J. Miller, *Phys. Rev. Lett.* **84**, 4617 (2000).

<sup>8</sup>A. O. Pecharsky, K. A. Gschneidner, Jr., V. K. Pecharsky, and C. E. Schindler, *J. Alloys Compd.* **338**, 126 (2002).

<sup>9</sup>V. K. Pecharsky, A. O. Pecharsky, and K. A. Gschneidner, Jr., *J. Alloys Compd.* **344**, 362 (2002).

<sup>10</sup>C. Ritter, L. Morellon, P. A. Algarabel, C. Magen, and M. R.

Ibarra, *Phys. Rev. B* **65**, 094405 (2002).

<sup>11</sup>H. F. Yang, G. H. Rao, W. G. Chu, G. Y. Liu, Z. W. Ouyang, and J. K. Liang, *J. Alloys Compd.* **339**, 189 (2002).

<sup>12</sup>L. Morellon, C. Ritter, C. Magen, P. A. Algarabel, and M. R. Ibarra, *Phys. Rev. B* **68**, 024417 (2003).

<sup>13</sup>V. K. Pecharsky, A. O. Pecharsky, Y. Mozharivskij, K. A. Gschneidner, Jr., and G. J. Miller, *Phys. Rev. Lett.* **91**, 207205 (2003).

<sup>14</sup>L. Morellon, Z. Arnold, C. Magen, C. Ritter, O. Prokhnenko, Y. Skorokhod, P. A. Algarabel, M. R. Ibarra, and J. Kamarad, *Phys. Rev. Lett.* **93**, 137201 (2004).

<sup>15</sup>Y. Mozharivskij, A. O. Pecharsky, V. K. Pecharsky, G. J. Miller, and K. A. Gschneidner, Jr., *Phys. Rev. B* **69**, 144102 (2004).

<sup>16</sup>C. Ritter, C. Magen, L. Morellon, P. A. Algarabel, M. R. Ibarra, V. K. Pecharsky, A. O. Tsokol, and K. A. Gschneider, Jr., *J. Phys.: Condens. Matter* **18**, 3937 (2006).

<sup>17</sup>A. O. Pecharsky, V. K. Pecharsky, and K. A. Gschneidner, Jr., *J. Alloys Compd.* **379**, 127 (2004).

<sup>18</sup>C. J. Voyer, D. H. Ryan, K. Ahn, K. A. Gschneidner, Jr., and V. K. Pecharsky, *Phys. Rev. B* **73**, 174422 (2006).

<sup>19</sup>H. F. Yang, G. H. Rao, G. Y. Liu, Z. W. Ouyang, W. G. Chu, W. F. Liu, X. M. Feng, and J. K. Liang, *J. Alloys Compd.* **348**, 150

- (2003).
- <sup>20</sup>V. K. Pecharsky and K. A. Gschneidner, Jr., *Adv. Mater.* (Weinheim, Ger.) **13**, 683 (2001).
- <sup>21</sup>E. M. Levin, V. K. Pecharsky, and K. A. Gschneidner, Jr., *Phys. Rev. B* **60**, 7993 (1999).
- <sup>22</sup>J. B. Sousa, M. E. Braga, F. C. Correia, F. Carpinteiro, L. Morellon, P. A. Algarabel, and M. R. Ibarra, *Phys. Rev. B* **67**, 134416 (2003).
- <sup>23</sup>J. B. Sousa, A. M. Pereira, F. C. Correia, J. M. Teixeira, R. P. Pinto, M. E. Braga, J. P. Araújo, L. Morellon, P. A. Algarabel, C. Magen, and M. R. Ibarra, *J. Phys.: Condens. Matter* **17**, 2461 (2005).
- <sup>24</sup>E. M. Levin, A. O. Pecharsky, V. K. Pecharsky, and K. A. Gschneidner, Jr., *Phys. Rev. B* **63**, 064426 (2001).
- <sup>25</sup>J. P. Araújo, A. M. Pereira, M. E. Braga, R. P. Pinto, F. C. Correia, J. M. Teixeira, J. B. Sousa, L. Morellon, P. A. Algarabel, C. Magen, and M. R. Ibarra, *J. Phys.: Condens. Matter* **17**, 4941 (2005).
- <sup>26</sup>A. M. Pereira, J. P. Araújo, M. E. Braga, R. P. Pinto, J. Ventura, F. C. Correia, J. M. Teixeira, J. B. Sousa, C. Magen, L. Morellon, P. A. Algarabel, and M. R. Ibarra, *J. Alloys Compd.* **423**, 66 (2006).
- <sup>27</sup>V. K. Pecharsky and K. A. Gschneidner, Jr., *J. Alloys Compd.* **260**, 98 (1997).
- <sup>28</sup>L. Morellon, J. Blasco, P. A. Algarabel, and M. R. Ibarra, *Phys. Rev. B* **62**, 1022 (2000).
- <sup>29</sup>Z. W. Ouyang, V. K. Pecharsky, K. A. Gschneidner, Jr., D. L. Schlagel, and T. A. Lograsso, *Phys. Rev. B* **74**, 094404 (2006).
- <sup>30</sup>C. Magen, P. A. Algarabel, L. Morellon, J. P. Araujo, C. Ritter, M. R. Ibarra, A. M. Pereira, and J. B. Sousa, *Phys. Rev. Lett.* **96**, 167201 (2006).
- <sup>31</sup>D. Haskel, Y. B. Lee, B. N. Harmon, Z. Islam, J. C. Lang, G. Srajer, Y. Mudryk, K. A. Gschneidner, Jr., and V. K. Pecharsky, *Phys. Rev. Lett.* **98**, 247205 (2007).
- <sup>32</sup>F. Holtzberg, R. J. Gambino, and T. R. McGuire, *J. Phys. Chem. Solids* **28**, 2283 (1967).
- <sup>33</sup>P. Schobinger-Papamantellos and A. Niggli, *J. Phys. Colloq.* **40**, 156 (1979).
- <sup>34</sup>N. P. Thuy, Y. Y. Chen, Y. D. Yao, C. R. Wang, S. H. Lin, J. C. Ho, T. P. Nguyen, P. D. Thang, J. C. P. Klaasse, N. T. Hien, and L. T. Tai, *J. Magn. Magn. Mater.* **262**, 432 (2003).
- <sup>35</sup>J. Rodríguez-Carvajal, *Physica B* **192**, 55 (1993).
- <sup>36</sup>D. T. Adroja, B. D. Rainford, J. M. de Teresa, A. del Moral, M. R. Ibarra, and K. S. Knight, *Phys. Rev. B* **52**, 12790 (1995).
- <sup>37</sup>David R. Lide, *CRC Handbook of Chemistry and Physics* (CRC, Boca Raton, FL, 2001).
- <sup>38</sup>J. Meyers, Scoot Chumbley, Wonyoung Choe, and Gordon J. Miller, *Phys. Rev. B* **66**, 012106 (2002).
- <sup>39</sup>C. Magen, L. Morellon, P. A. Algarabel, C. Marquina, and M. R. Ibarra, *J. Phys.: Condens. Matter* **15**, 2389 (2003).
- <sup>40</sup>C. Magen, L. Morellon, Z. Arnold, P. A. Algarabel, C. Ritter, M. R. Ibarra, J. Kamarad, A. O. Tsokol, K. A. Gschneidner, Jr., and V. K. Pecharsky, *Phys. Rev. B* **74**, 134427 (2006).
- <sup>41</sup>G. J. Miller, *Chem. Soc. Rev.* **35**, 799 (2006).
- <sup>42</sup>Jens Jensen and Allan R. Mackintosh, *Rare Earth Magnetism* (Clarendon, Oxford, 1991).
- <sup>43</sup>C. Magen, C. Ritter, L. Morellon, P. A. Algarabel, M. R. Ibarra, A. O. Tsokol, K. A. Gschneidner, Jr., and V. K. Pecharsky, *Phys. Rev. B* **74**, 174413 (2006).